Erschienen in: SiliconPV 2019, The 9th International Conference on Crystalline Silicon Photovoltaics : 8-10 April 2019, Leuven, Belgium / Poortmans, Jef et al. (Hrsg.). - Melville, New York : AIP Publishing, 2019. - (AIP Conference Proceedings ; 2147,1). - 140011. - ISBN 978-0-7354-1892-9
http://dx.doi.org/10.1063/1.5123898

Does LeTID Occur in c-Si Even Without a Firing Step?

David Sperber[a)], Florian Furtwängler[b)], Axel Herguth[c)], and Giso Hahn[d)]

University of Konstanz, Department of Physics, 78457 Konstanz, Germany

[a)]Corresponding author: david.sperber@uni-konstanz.de
[b)]fw@schwarzwald-gymnasium.de
[c)]axel.herguth@uni-konstanz.de
[d)]giso.hahn@uni-konstanz.de

Abstract. It is shown that a non-fired B-doped floatzone silicon sample coated with SiN_x:H may show severe bulk related degradation and regeneration during illuminated treatment at elevated temperature. It is discussed that the likely cause is light and elevated temperature induced degradation (LeTID) in the silicon bulk. Firing is found to modulate the extent of LeTID so that degradation may either be weaker or stronger compared to the non-fired sample depending on firing parameters. A sample which was annealed instead of fired is found to be stable for up to 1,000 h of treatment time.

INTRODUCTION

Light and elevated temperature induced degradation (LeTID) was first observed in multicrystalline silicon (mc-Si) [1-3] but later described to likely affect floatzone silicon (FZ-Si) [4-7] and Czochralski silicon (Cz-Si) [8-10] as well. An overview of light-induced degradation properties in FZ-Si and mc-Si is shown in Tab. 1 and illustrates the great similarity of both phenomena. As degradation in both materials can furthermore be triggered by either illumination or elevated temperature on their own [1,11,12], LeTID appears to be an appropriate phenomenological terminology for degradation in both materials. For a detailed discussion on the occurrence of LeTID in different types of crystalline silicon, the reader is referred to [12].

It is well known that the occurrence of LeTID is strongly influenced by fast firing parameters such as (measured) peak firing temperature T_{fire} [4,5,13,14] and the shape of the firing profile [4,15]. Furthermore, it was shown earlier that a non-fired sample did not degrade significantly [16]. Thus, it is often assumed that a firing step is necessary for the emergence of LeTID. In contrast to this belief, the present study shows that LeTID may affect a non-fired sample as well. Furthermore, the effects of different firing conditions or annealing instead of firing are investigated. Part of the data was already presented earlier [17]. However, neither the strength of degradation nor the link to LeTID had been fully understood at the time of the original publication and the present study thus aims to provide a more complete picture.

EXPERIMENTAL

Samples were made of B-doped FZ-Si wafers (doping density $N_{\mathrm{d}} = 1.5 \cdot 10^{16}$ cm^{-3}, thickness $d = 250$ µm) which had already received chemical cleaning by the manufacturer and were shipped with a thin (~1 nm) chemically grown silicon oxide layer on top. On two samples ("fired med" and "fired high"), this "original" silicon oxide layer (SiO_x type 1) was left in place whereas the other samples received cleanings in HCl (37%), followed by oxidation at 50°C in a solution of deionized water, NH_3 (25%) and H_2O_2 (30%) mixed in a ratio 9.5:1:2, followed by oxidation at 65°C in a solution of deionized water, HCl (37%) and H_2O_2 (30%) mixed in a ratio 8:1:1. Each of these oxidation steps was followed by a dip in diluted HF (2%). Finally, a thin chemical oxide (SiO_x type 2) was grown by another oxidation at 80°C in a solution of deionized water, HCl (37%) and H_2O_2 (30%) mixed in a ratio 8:1:1.

TABLE 1. Properties of light and elevated temperature induced degradation in FZ- and mc-Si. A detailed discussion can be found in [12].

Property	FZ-Si	mc-Si
Firing temperature	T_{fire} ↑, ΔN_{eff} ↑ [4,5,18]	T_{fire} ↑, ΔN_{eff} ↑ [13,14,16]
Firing profile	Cooling rate ↑, ΔN_{eff} ↑ [4]	Cooling rate ↑, ΔN_{eff} ↑ [15]
Sample thickness	d ↑, ΔN_{eff} ↑ [4]	d ↑, ΔN_{eff} ↑ [19]
Dielectric layers	Strong impact [5,7]	Strong impact [2,20]
Base material	Strong impact [4,5]	Strong impact [1,13,21]
$k = \tau_p/\tau_n$	18-45 [5,22,23]	13-36 [6,13,24,25]
$k = k(t)$	Yes [12]	Yes [26]
Regeneration	Yes [4,5,18]	Yes [3,26-28]
Partial reversibility	Yes [22,23]	Yes [29,30]
Carrier-induced	Yes [12]	Yes [3,27,31]
Time scale	Rather short [4,5]	Rather long [1,28]

Thus, all samples investigated in this study feature a thin (~1 nm) chemically grown SiO_x layer albeit from two different sources. It should be noted that SiO_x types 1 and 2 have lead to very similar degradation in the past (data not shown) and are thus not expected to cause significant differences in sample behavior. In a next step, samples were coated with ~75 nm of SiN_x:H in an "Oxford Instruments Plasmalab 100" direct plasma-enhanced chemical vapor deposition tool (13.56 MHz) using SiH_4 (gas flow 11 sccm), NH_3 (13 sccm) and N_2 (996 sccm) as precursor gases. Deposition was carried out at 400°C for 110 s. Including heat-up (7 min) before and gas removal (2 min) after deposition, a sample was subjected to elevated temperature in the process chamber for ~11 min. A "non-fired" sample received no further temperature treatment. Samples "fired low", "fired med", and "fired high" were fired in two different furnaces with firing profiles as shown in Fig. 1. One sample was "annealed" instead of fired in N_2 atmosphere at 420°C for 30 min.

Samples were then subjected to treatments at elevated temperature (75°C or 80°C) on hotplates under halogen lamp illumination (0.6 or 1 suns). The term "1 sun" refers to an illumination intensity which leads to the same short circuit current I_{sc} in a solar cell under halogen lamp illumination compared to its I_{sc} in an AM1.5 solar spectrum simulator (for further details see [32]). During treatment, samples were repeatedly taken off a hotplate to measure the effective excess charge carrier lifetime τ_{eff} with a "Sinton Instruments WCT-120" lifetime tester at 30°C. Values of the surface related saturation current density J_0 [12,33] were extracted according to the method described in [34]. The change in effective defect density ΔN_{eff} was calculated with reference to the measurement after $t_0 = 2$ min of treatment according to

$$\Delta N_{eff} = \frac{1}{\tau_{LeTID}(t)} = \frac{1}{\tau_{eff}(t)} - \frac{1}{\tau_{eff}(t_0)} \quad (1)$$

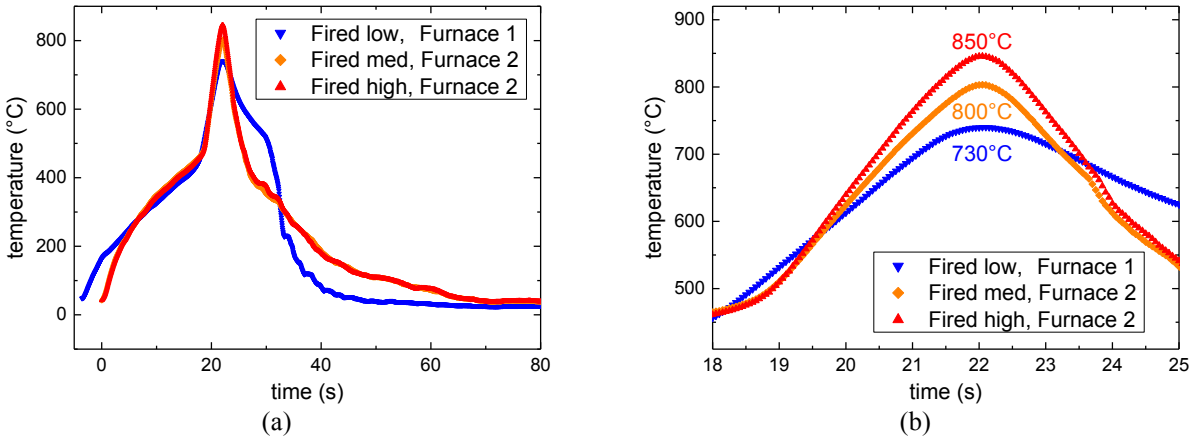

FIGURE 1. Temperature profile during firing as measured by a type K thermocouple which was pressed onto a sample's surface by mechanical prestress. Two different fast firing furnaces were used which differ mainly in the cool-down ramp as is evident in the measured profiles. The time axis of the measurement in Furnace 1 was shifted such that all maxima coincide.

RESULTS

Figure 2 shows time- and injection-resolved τ_{eff} data ranging from low excess carrier density $\Delta n = 3 \cdot 10^{14}$ cm^{-3} shown in blue to high $\Delta n = 1 \cdot 10^{16}$ cm^{-3} shown in red. As can be seen, the non-fired sample (a) shows significant changes of τ_{eff} during treatment at 75°C and 0.6 suns. A first minimum after ~5 h of treatment is especially pronounced at low injection (blue) whereas a long-term degradation is most limiting at high injection (red). It has been shown before that a very similar first degradation feature arises from bulk related degradation and regeneration in fired samples [4,5,12] and is most likely related to LeTID as discussed before (Tab. 1). A very similar long-term decline, on the other hand, has been shown to result from surface related degradation (SRD) and is discussed in detail elsewhere [12,35-37]. It thus appears very likely that the non-fired sample is affected by LeTID and SRD during treatment at elevated temperature and illumination. This assignment is further verified by the evolution of J_0 values which will be discussed later on. Compared to the non-fired sample, a sample "fired low" (b) reaches higher levels of τ_{eff} (note the different scale) and shows a weaker degree of LeTID. As the only difference between both samples is the firing step, it can be concluded that firing at "low" conditions has decreased the strength of LeTID.

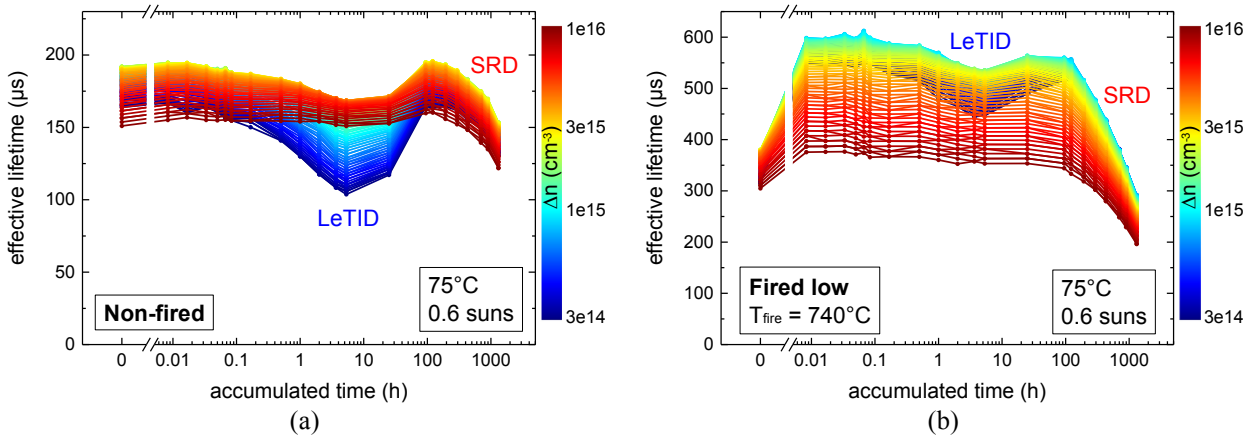

FIGURE 2. Time-and injection-resolved τ_{eff} of (a) the "non-fired" and (b) the "fired low" sample during treatment at 75°C and 0.6 suns. Colors relate to Δn ranging from $3 \cdot 10^{14}$ cm^{-3} (blue) to $1 \cdot 10^{16}$ cm^{-3} (red). Part of data shown in [17].

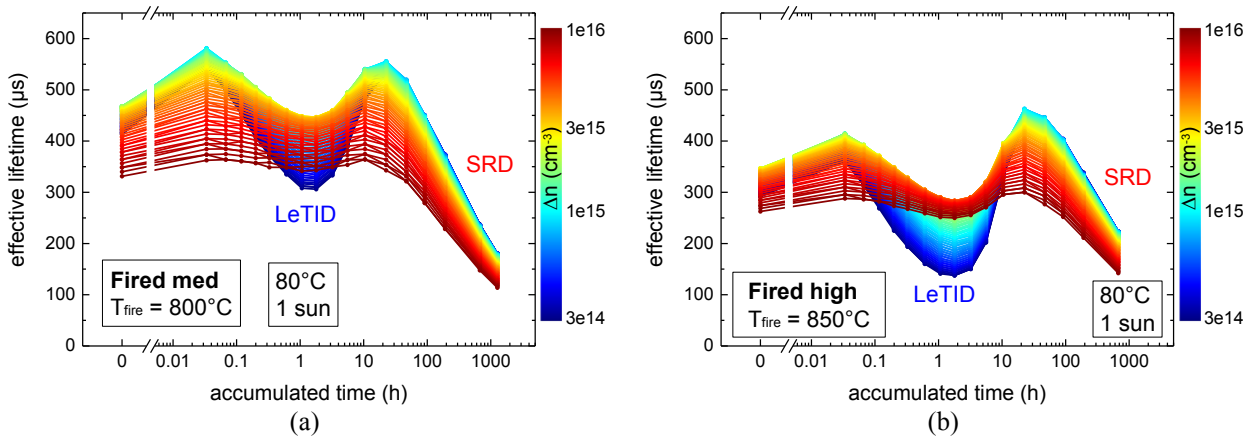

FIGURE 3. Time- and injection-resolved τ_{eff} of (a) the "fired med" and (b) the "fired high" sample during treatment at 80°C and 1 sun. Part of data shown in [7].

As expectable from Tab. 1, firing at higher temperatures and with steeper cool-down ramps (Fig. 1) leads to stronger LeTID in the samples shown in Fig. 3. Compared to Fig. 2, the samples degrade slightly faster due to stronger illumination and slightly increased temperature during treatment. Annealing instead of firing, on the other hand, results in very stable τ_{eff} according to Fig. 4 (a). A possible explanation is that the sample has already completed the cycle of degradation and recovery both in the bulk and at the surface during annealing at 420°C and is therefore stable for up to 1,000 h of sample treatment. A comparison of J_0 values in Fig. 4 (b) furthermore reveals a good surface passivation of the annealed sample whereas especially the non-fired sample is not well passivated which explains its overall lower level of τ_{eff}. While J_0 values are rather stable during the first hours of treatment, all samples but the annealed one show a strong increase of J_0 after longer treatment time indicating SRD. As SRD is a carrier-induced degradation mechanism [36] just like LeTID, the samples "fired med" and "fired high" show an earlier rise of J_0 due to the slightly harsher treatment conditions (stronger illumination, higher treatment temperature).

Given the differences in passivation quality, it is useful to calculate the change in effective defect density ΔN_{eff} according to Eq. 1 for a better comparison of LeTID extent. As can be seen in Fig. 5, the non-fired sample shows rather strong LeTID whereas the samples "fired low" and "fired med" show less LeTID. However, the highest ΔN_{eff} is achieved by the sample "fired high". Accordingly, it appears that a firing step is not causing but rather modulating the extent of LeTID in the given samples. Annealing, on the other hand, results in very low ΔN_{eff} which may not even be related to LeTID given the rather constant injection dependency shown in Fig. 4 (a).

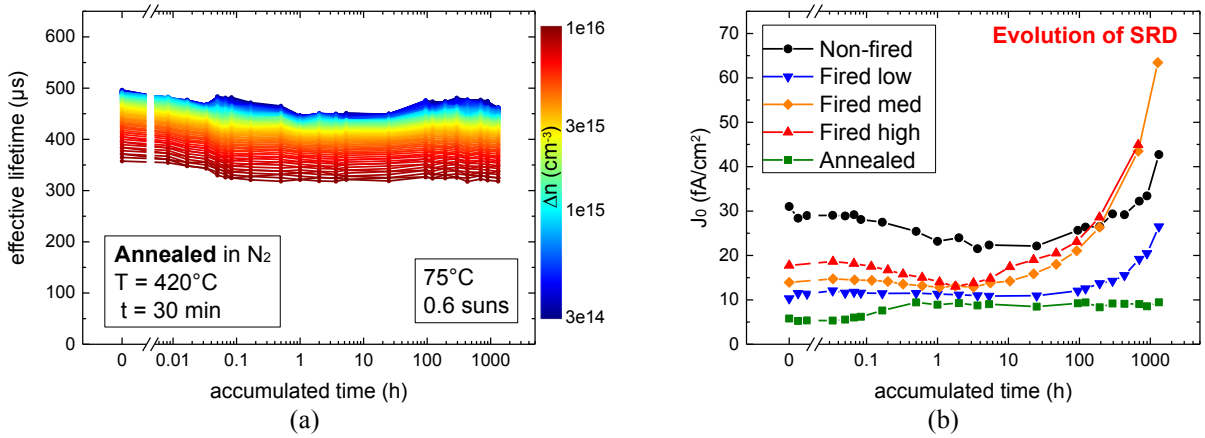

FIGURE 4. (a) Time- and injection-resolved τ_{eff} of the "annealed" sample during treatment at 75°C and 0.6 suns. Part of data shown in [17]. (b) Evolution of J_0 during the treatments shown in Figs. 2-4.

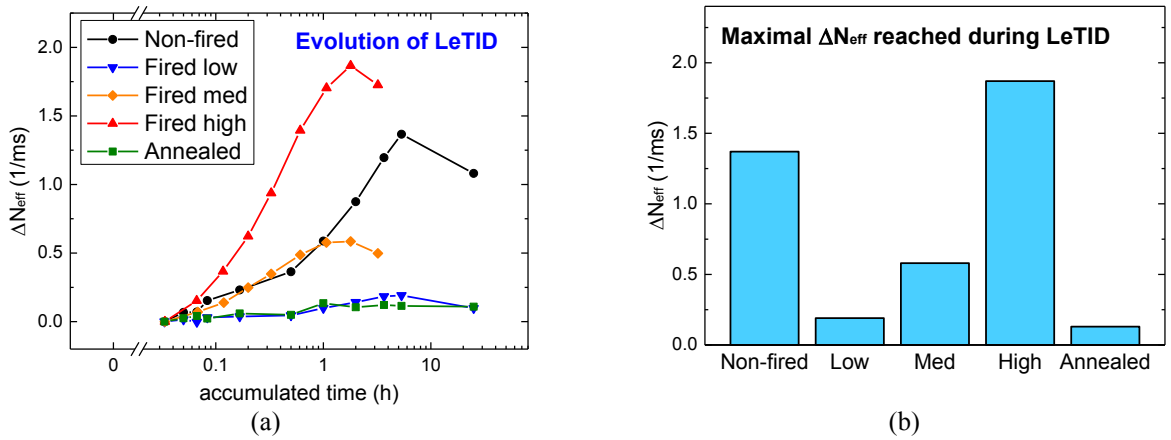

FIGURE 5. (a) Evolution of ΔN_{eff} (at $\Delta n = 0.1 \cdot N_d$) during the treatments shown in Figs. 2-4. (b) Maximal values of ΔN_{eff} reached during LeTID.

CONCLUSIONS

It has been shown that a non-fired sample may be strongly affected by LeTID. Firing at different temperatures and with different firing profiles resulted in a modulation of the LeTID extent so that both weaker and stronger LeTID could be achieved compared to the non-fired sample. While the results presented in this study indicate that a firing step is not necessarily needed for the occurrence of LeTID, it still remains well possible that LeTID is a hydrogen-induced degradation phenomenon as proposed by many different authors (*e.g.*, [13,15,26,28,37]). It appears particularly possible that a SiN_x:H deposition step carried out at 400°C already introduces enough hydrogen into the silicon bulk to cause significant LeTID. Interestingly, annealing at a similar temperature of 420°C has resulted in a very stable sample. As annealing was, however, performed for a significantly longer time period (30 min), it appears possible that hydrogen or another defect precursor has either diffused towards the surface or switched to more stable bonding states during the annealing treatment whereas it might not have had the time to do so during the rather short time (~4 min) at elevated temperature during and after deposition of SiN_x:H.

ACKNOWLEDGMENTS

The authors would like to thank A. Graf, L. Mahlstaedt, S. Joos, B. Rettenmaier, L. Kraus, and J. Engelhardt for technical support. Part of this work was supported by the German Federal Ministry for Economic Affairs and Energy under contract numbers FKZ: 0324001 and 0324204B.

REFERENCES

1. K. Ramspeck, S. Zimmermann, H. Nagel, A. Metz, Y. Gassenbauer, B. Birkmann, and A. Seidl, "Light induced degradation of rear passivated mc-Si solar cells," in *Proc. 27th EUPVSEC* (Frankfurt a. M., Germany, 2012), pp. 861-865.
2. F. Fertig, K. Krauß, and S. Rein, Phys. Status Solidi RRL **9**, 41-46 (2015).
3. F. Kersten, P. Engelhart, H. C. Ploigt, A. Stekolnikov, T. Lindner, F. Stenzel, and J. W. Müller, Sol. Energy Mater. Sol. Cells **142**, 83-86 (2015).
4. D. Sperber, A. Heilemann, A. Herguth, G. Hahn, IEEE J. Photovoltaics **7**, 463-470 (2017).
5. T. Niewelt, M. Selinger, N. E. Grant, W. Kwapil, J. D. Murphy, and M. C. Schubert, J. Appl. Phys. **121**, 185702 (2017).
6. T. Niewelt, F. Schindler, W. Kwapil, R. Eberle, J. Schön, M. C. Schubert, Prog. Photovolt. Res. Appl. **26**, 533-542 (2018).
7. D. Sperber, A. Herguth, and G. Hahn, "Investigating possible causes of light induced degradation in boron-doped float-zone silicon," in *Proc. 33rd EUPVSEC* (Amsterdam, The Netherlands, 2017), pp. 565-568.

8. F. Fertig, R. Lantzsch, A. Mohr, M. Schaper, M. Bartzsch, D. Wissen, F. Kersten, A. Mette, S. Peters, A. Eidner, J. Cieslak, K. Duncker, M. Junghänel, E. Jarzembowski, M. Kauert, B. Faulwetter-Quandt, D. Meißner, B. Reiche, S. Geißler, S. Hörnlein, C. Klenke, L. Niebergall, A. Schönmann, A. Weihrauch, F. Stenzel, A. Hofmann, T. Rudolph, A. Schwabedissen, M. Gundermann, M. Fischer, J. W. Müller, D. J. W. Jeong, Energy Procedia **124**, 338–345 (2017).
9. D. Chen, M. Kim, B. V. Stefani, B. J. Hallam, M. D. Abbott, C. E. Chan, R. Chen, D. N. R. Payne, N. Nampalli, A. Ciesla, T. H. Fung, K. Kim, S. R. Wenham, Sol. Energy Mater. Sol. Cells **172**, 293-300 (2017).
10. D. Sperber, A. Schwarz, A. Herguth, and G. Hahn, Phys. Status Solidi A **215**, 1800741, (2018).
11. C. E. Chan, D. N. R. Payne, B. J. Hallam, M. D. Abbott, T. H. Fung, A. M. Wenham, B. S. Tjahjono, and S. R. Wenham, IEEE J. Photovoltaics **6**, 1473-1479 (2016).
12. D. Sperber, "Bulk and surface related degradation phenomena in monocrystalline silicon at elevated temperature and illumination," Doctoral dissertation, University of Konstanz, submitted.
13. K. Nakayashiki, J. Hofstetter, A. E. Morishige, T.-T. A. Li, D. B. Needleman, M. A. Jensen, and T. Buonassisi, IEEE J. Photovoltaics **6**, 860-868 (2016).
14. D. Bredemeier, D. Walter, S. Herlufsen, and J. Schmidt, AIP Adv. **6**, 35119 (2016).
15. R. Eberle, W. Kwapil, F. Schindler, M. C. Schubert, and S. W. Glunz, Phys. Status Solidi RRL **10**, 861-865 (2016).
16. C. E. Chan, D. N. R. Payne, B. J. Hallam, M. D. Abbott, T. H. Fung, A. M. Wenham, B. S. Tjahjono, and S. R. Wenham, IEEE J. Photovoltaics **6**, 1473-1479 (2016).
17. D. Sperber, F. Furtwängler, A. Herguth, and G. Hahn, "On the stability of dielectric passivation layers under illumination and temperature treatment," in *Proc. 32nd EUPVSEC* (Munich, Germany, 2016), pp. 523-526.
18. D. Sperber, A. Herguth, and G. Hahn, Energy Procedia **92**, 211-217 (2016).
19. D. Bredemeier, D. C. Walter, and J. Schmidt, Sol. RRL **2**, 1700159 (2018).
20. F. Kersten, J. Heitmann, and J. W. Müller, Energy Procedia **92**, 828-832 (2016).
21. J. M. Fritz, A. Zuschlag, D. Skorka, A. Schmid, and G. Hahn, Energy Proc.edia **124**, 718-725 (2017).
22. D. Sperber, A. Herguth, and G. Hahn, Phys. Status Solidi RRL **11**, 1600408 (2017).
23. N. Grant, F. E. Rougieux, D. Macdonald, J. Bullock, and Y. Wan, J. Appl. Phys. **117**, 55711 (2015).
24. D. Bredemeier, D. Walter, S. Herlufsen, and J. Schmidt, Energy Procedia **92**, 773-778 (2016).
25. A. E. Morishige, M. A. Jensen, D. B. Needleman, K. Nakayashiki, J. Hofstetter, T.-T. A. Li, and T. Buonassisi, IEEE J. Photovoltaics **6**, 1466-1472 (2016).
26. M. A. Jensen, A. E. Morishige, J. Hofstetter, D. B. Needleman, and T. Buonassisi, IEEE J. Photovoltaics **7**, 980-987 (2017).
27. D. N. R. Payne, C. E. Chan, B. J. Hallam, B. Hoex, M. D. Abbott, S. R. Wenham, and D. M. Bagnall, Sol. Energy Mater. Sol. Cells **158**, 102-106 (2016).
28. A. Zuschlag, D. Skorka, and G. Hahn, Prog. Photovoltaics Res. Appl. **25**, 545-552 (2017).
29. T. Luka, S. Großer, C. Hagendorf, K. Ramspeck, and M. Turek, Sol. Energy Mater. Sol. Cells **158**, 43-49 (2016).
30. T. H. Fung, M. Kim, D. Chen, C. E. Chan, B. J. Hallam, R. Chen, D. N. R. Payne, A. Ciesla, S. R. Wenham, M. D. Abbott, Sol. Energy Mater. Sol. Cells **184**, 48-56 (2018).
31. W. Kwapil, T. Niewelt, and M. C. Schubert, Sol. Energy Mater. Sol. Cells **173**, 80-84 (2017).
32. A. Herguth, Energy Procedia **124**, 53-59 (2017).
33. K. McIntosh and L. Black, J. Appl. Phys **116**, 14503 (2014).
34. A. Kimmerle, J. Greulich, and A. Wolf, Sol. Energy Mater. Sol. Cells **142**, 116-122 (2015).
35. D. Sperber, A. Graf, D. Skorka, A. Herguth, and G. Hahn, IEEE J. Photovoltaics **7**, 1627-1634 (2017).
36. D. Sperber, A. Schwarz, A. Herguth, and G. Hahn, Sol. Energy Mater. Sol. Cells **188**, 112-118 (2018).
37. K. Kyung, R. Chen, D. Chen, P. Hamer, A. Ciesla née Wenham, S. Wenham, Z. Hameiri, IEEE J. Photovoltaics **9**, 97-105 (2019).
38. A. Ciesla, S. Wenham, R. Chen, C. Chan, D. Chen, B. Hallam, D. Payne, T. Fung, M. Kim, S. Liu, S. Wang, K. Kyung, A. Samadi, C. Sen, C. Vargas, U. Varshney, B. V. Stefani, P. Hamer, G. Bourret-Sicotte, N. Nampalli, Z. Hameiri, C. Chong, A. Malcolm, "Hydrogen-induced degradation," in *Proc. 7th WCPEC* (Waikoloa, Hawaii, 2018), pp. 1-8.